CHARACTERIZATION OF MOLECULAR CLOUD STRUCTURE

V. OSSENKOPF, F. BENSCH, & J. STUTZKI
1. Physikalisches Institut der Universität zu Köln, Zülpicher Straße 77, 50937 Köln, Germany
E-mail: ossk@zeus.ph1.uni-koeln.de

The complexity of observed molecular cloud structures prevents any simple description and complicates the comparison of observations with cloud models. We provide a short overview on the techniques that are applied to parameterize the cloud structure. Several independent parameters have to be combined including measures for the isotropic density or intensity scaling behaviour, the degrees of anisotropy, the structure in velocity space and the relation between density and velocity structure. Deviations from a general self-similar behaviour provide the clue to estimate the relative influence of different physical processes driving structure formation and thus to understand the turbulent nature of molecular clouds.

1 Introduction

Observations of molecular clouds show a complex, filamentary and often self-similar structure over a wide range of spatial scales. With the radio telescopes and interferometers available today, extended maps in molecular lines have been obtained providing large data cubes of intensities at two celestial and one velocity coordinate (e.g. Dame 1999). In addition many clouds have been observed in their far infrared continuum emission or in the near infrared extinction. But the lack of velocity information in these observations further complicates the derivation of the cloud turbulence structure here.

For demonstration we show the Polaris Flare in Fig. 1, a high galactic latitude molecular cloud without star formation that we will use as a well studied example throughout this paper. The figure shows three integrated line maps at different spatial resolutions observed with the CfA 1.2m telescope in ^{12}CO 1-0 (Heithausen & Thaddeus 1990), with the KOSMA 3m telescope in ^{12}CO 2-1 (see Bensch et al. 1999), and with the IRAM 30m telescope (Falgarone et al. (1998), we show only the ^{12}CO 1-0 results here). The observations cover a dynamical range in linear resolution from about 50 pc down to 0.01 pc.

A direct deduction of the three-dimensional density, temperature, and velocity structure from observed data cubes is however impossible and a cloud simulation is required to fit the observed properties by a physically justified cloud structure. Simulations were done using empirical fractal models (Ossenkopf et al. 1998) or hydrodynamic and magnetohydrodynamic mod-

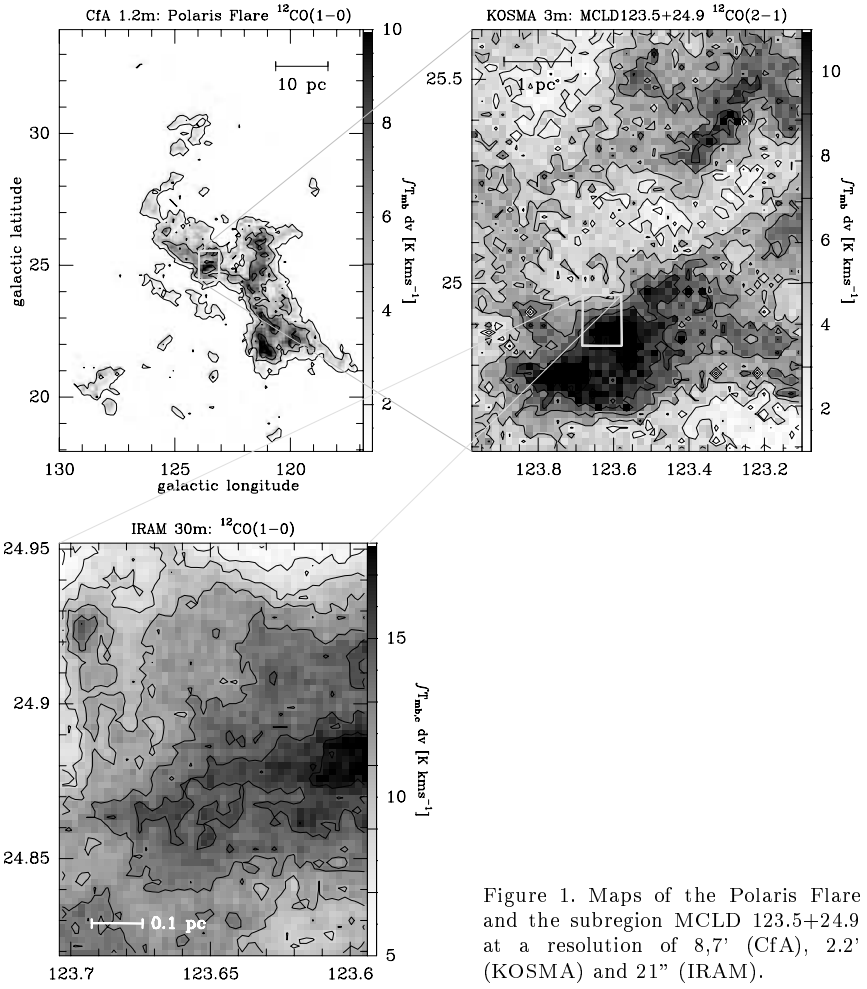

Figure 1. Maps of the Polaris Flare and the subregion MCLD 123.5+24.9 at a resolution of 8,7' (CfA), 2.2' (KOSMA) and 21" (IRAM).

els (see e.g. Mac Low et al. 1998, Padoan et al. 1998, Ostriker et al. 1998, Vázquez-Semadeni et al. 1999). A major stumbling block in this fit is the lack of sufficiently reliable parameters characterizing both the observed and the simulated structure. For complex molecular cloud structures a geometrical description is no longer meaningful. The simulations can never provide an exact reproduction of the observed cubes but only reproduce the general statistical properties like scaling relations. We need statistical methods to an-

alyze the data cubes. The methods have to provide few easily understandable parameters representing as much information as possible about the properties of an observed data cube. Unfortunately, our knowledge about the physics of turbulence in molecular clouds is still insufficient to discriminate at this point which observational parameters are most relevant for certain physical questions or might be translated into physical parameters. Hence, we have to deal with a relatively large number of methods all showing a somewhat different perspective of molecular cloud structure.

As shown by Combes (this volume) and in Sect. 3 we find self-similar relations within a relatively large size range. We expect, however, that physical processes like molecular energy dissipation, the onset of star formation, MHD waves, and outflows with their characteristic size scales will show up in the structure as departures from a self-similar behaviour. First promising results in the search for such departures were obtained by Blitz & Williams (1997) who found a change in the slope of the clump distribution function at small scales in a star-forming cloud and by Goodman et al. (1998) finding a flattening of the size-line width relation in dense cores. Both results still need further confirmation by complementary observations. A comprehensive discussion of the corresponding implications for the understanding of star-formation was given by Williams et al. (1999).

2 Basic restrictions

Useful algorithms for the structure determination have to be applicable with the same reliability both to the observations and the simulations with their respective limitations. Hydrodynamic and magnetohydrodynamic models are mainly restricted by the numerical resolution of at most a few hundred grid points in each dimension but provide the full three-dimensional density and velocity structure. Their structure is often characterized in terms of the probability density function (PDF) of densities and velocities but both are not easily obtained for observed clouds.

Besides their lower dimensionality observations are limited by a finite signal-to-noise ratio (S/N) which seems to create artificial structure at the smallest scales, the finite resolution of each telescope which wipes out structure even at scales somewhat beyond the HPBW of the telescope, and the limited map size restricting the available dynamical range.

For a direct comparison, the observable intensity data cubes have to be computed from the model structures including all observational effects. In case of optically thin lines in a medium with uniform excitation temperature, this includes a simple projection of the density weighted velocity component

in the line of sight. The effects of this projection are discussed in detail by Mac Low & Ossenkopf (1999) and Vázquez-Semadeni (this volume). In general one has to take the full radiative transfer problem into account which provides an additional level of complication (Juvela 1999, Ossenkopf et al. 1999).

3 Measures of the structure scaling behaviour

The methods to characterize the scaling behaviour of the intensity structure can be divided into two families. The first set of analysis tools starts from the picture of an interstellar cloud as a continuous compressible medium with transient fluctuations and fractal or multifractal properties as discussed by Combes (this volume).

Measures of the fractal dimension or fractal scaling relations were introduced for astrophysical maps with the area-perimeter relation of iso-intensity contours (Falgarone et al. 1991, Vogelaar & Wakker 1994), the box-counting fractal dimension (Zimmermann & Stutzki 1993), and the structure-tree analysis (Houlahan & Scalo 1992). Extensions to multifractal properties have been proposed by Chappell & Scalo (1992). We have tested the area-perimeter fractal dimension and the box-counting dimension for simulated maps and found them to be extremely sensitive to noise in the data so that they should be computed only for maps with a very good S/N.

Another approach studies the spectrum of intensity fluctuations depending on their size. Measurements of the power spectrum date back to investigations from e.g. Stenholm (1984). A major problem in this analysis is however the artificial periodic continuation introduced by the Fourier transform which can create artificial edges if a map does not trace the full extent of emission from a molecular cloud. The Δ-variance introduced by Stutzki et al. (1998) turns out to be a more reliable function. It contains all information from the power spectrum, does not require a Fourier transform, and can easily separate observational effects like noise and beam-smearing from internal cloud properties. The method was carefully tested by Bensch et al. (1999) and the results from its application to the Polaris Flare maps are shown in Fig. 2. All curves are reasonably represented by power laws but the index changes smoothly from 0.6 at the largest scale to 1.3 at the smallest scales. For the full scale range this means a noticeable deviation from a self-similar behaviour. Future extensions of these approaches might include the principal component analysis discussed in Sect. 5 and wavelet analysis methods (Langer et al. 1993).

The second family of methods is based on the physical picture of molecular clouds as a two-phase medium where dense clumps are partially confined by the interclump gas pressure. The algorithms search for coherent units

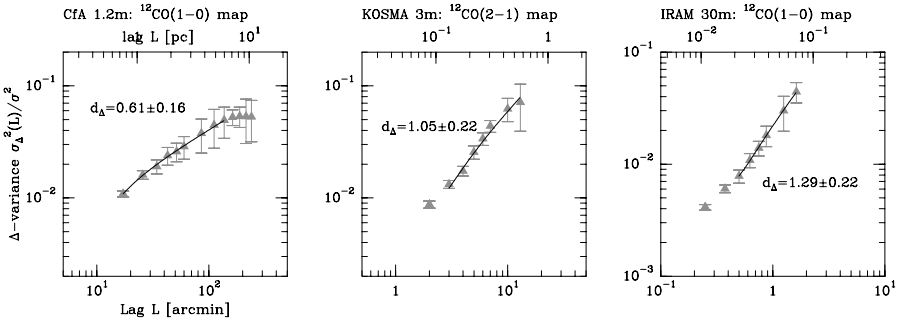

Figure 2. Δ-variance spectra for the Polaris Flare maps in Fig. 1. The Δ-variance is a measure for the relative structural variation at a certain spatial scale. The solid lines represent power law fits with corrections for noise and beam smearing.

in position-velocity space. Stutzki et al. (1998) have shown, however, that there is no strict separation between the two families since a superposition of many clumps with a power-law size and density spectrum turns out to be equivalent to a continuous fractal structure. Clump decomposition algorithms were introduced by Stutzki & Güsten (1990, `GAUSSCLUMPS`) and by Williams et al. (1994, `CLUMPFIND`). For most clumps both methods are equivalent, the number of small clumps is however overestimated by `GAUSSCLUMPS` and underestimated by `CLUMPFIND` (Williams et al. 1999).

Heithausen et al. (1998) have applied `GAUSSCLUMPS` to the Polaris Flare observations. They find unique power laws interconnecting the full range of scales for the number-size relation and the size-mass relation of the clumps. The resulting combined number-mass relation is shown in Fig. 3. This result seems to indicate a perfectly self-similar behaviour. The power-law indices for the clump spectra can be translated into an equivalent exponent of the Δ-variance of 0.78. If we introduce a correction to the mass-size relation taking into account that the conversion factor between clump mass and CO intensity is influenced by optical depth effects the equivalent exponent changes to about 1.1...1.3.

Nevertheless, the clump decomposition suggests self-similarity while Δ-variance analysis and the eye-inspection of the integrated maps reveals deviations from self-similarity. The solution to this contradiction must be hidden in the velocity structure which is only seen by the clump decomposition algorithms.

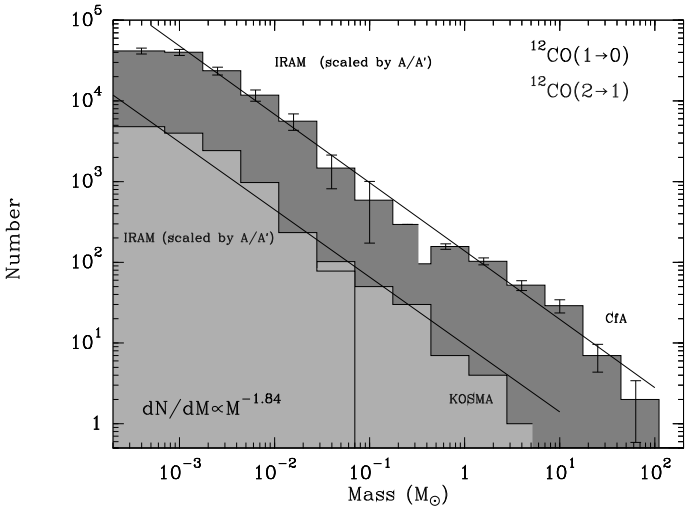

Figure 3. Clump mass spectrum for the Polaris Flare determined from CO 1-0 (top histogram) and 2-1 observations (bottom). The straight lines show a power law fit to the data (from Heithausen et al. 1998).

4 Measures of anisotropy

The tools to characterize the general scaling behaviour and fractal structure will necessarily fail in situations with strong anisotropies created e.g. by shock fronts, shells and outflows. Anisotropies and general filamentary properties have to be detected by some kind of asymmetry functions.

One measure has been introduced by Adams & Wiseman (1994) with the ratio between the squared maximum diameter and the area of iso-intensity contours. It was successfully applied to filamentary IRAS maps by Wiseman & Adams (1994) but cannot discriminate between different anisotropic structures like sheets, strings, shock bows or shells. When looking for a certain type of anisotropic structures it is probably more convenient to use algorithms detecting exactly those structures (see e.g. Forbes & Thomson 1992).

We found that many types of anisotropy are easily characterized in Fourier space and favour the application of the Δ-variance analysis and similar methods on the power spectrum, although this implies the general Fourier transform problems discussed above. This method can discriminate between different degrees of anisotropy at different scales and thus separate large-scale streams, small shock structures, and shells. Further systematic studies have

to be done in this field to establish a few sets of reliable parameters characterizing anisotropy in molecular clouds.

5 The structure in velocity space

A huge amount of information is hidden in the measurable velocity structure. There are numerous attempts to deduce the velocity PDF from observations. Falgarone & Phillips (1990) have estimated velocity PDFs from high S/N observations of single line profiles. Investigating the statistical moments of profiles Falgarone et al. (1994) found non-Gaussian wings for many observations and provided a first comparison with hydrodynamic simulations. Unfortunately, the method is only reliable for optically thin transitions at a very high S/N. Another approach to the velocity PDFs including the spatial correlation was introduced by Kleiner & Dickmann (1985) and considerably improved by several authors (see Miesch et al. 1999). They computed the spatial distribution of line velocity centroids avoiding some problems of optical depth effects and noise. However, the higher order moments of the distribution are very sensitive to distortions of the baseline and non-Gaussian noise.

A traditional measure for the spatial velocity distribution is the size-line width relation for clouds and clumps introduced by Larson (1981) and performed by many other observers (see also Vázquez-Semadeni in this volume). A comprehensive recent overview including a careful estimate of many possible errors was given by Goodman et al. (1998). Most studies obtain power laws $\Delta v_{obs} \propto R^{\gamma}$ with $\gamma = 0.35 \ldots 0.7$ over wide spatial ranges.

A major problem in the computation of these size-line width relations is the need for well separated entities in position-velocity space providing definite values for a size and line width. Alternatively one can obtain the average drift behaviour in velocity space by computing size-line width relations from a measurement of the average line width within (virtual) telescope beams of varying size, i.e. of the intensity weighted velocity dispersion within a certain radius. Here, we face the problem that the velocity dispersion is determined by two different scales - the cloud depth traced by the line of sight which shows up as the local line width in one point and the size of the virtual beam that we consider. To separate the two effects we have applied the analysis both to the total velocity dispersion within the virtual beam and to the dispersion of the velocity centroids only. Results for the Polaris Flare observations are shown in Fig. 4. The relation based on velocity centroids is a unique power law over four orders of magnitude with a slope $\gamma = 0.42$ which is close to the original Larson coefficient of 0.38. The curves for the total line width within the beam show that these are dominated by the line-of-sight integration up to

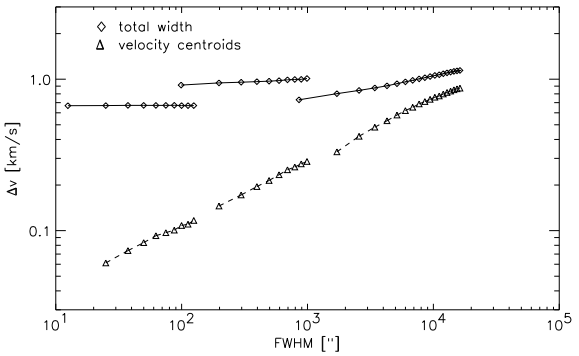

Figure 4. Size-line width relations for the Polaris Flare observations with IRAM (smallest scales), KOSMA, and the CfA 1.2m telescope (largest scale). The deviation of the KOSMA data for the full line width relations is probably due to the lower S/N of these observations.

the largest scales. More information on the drift behaviour in velocity space can be obtained from the investigation of the PDF of velocity increments (Miesch & Scalo 1995, Lis et al. 1998, Miesch et al. 1999).

Other methods to consider the spatial variation of the line profiles include e.g. the application of the Δ-variance analysis in velocity space and for velocity channel maps (Mac Low & Ossenkopf 1999) and the investigation of the spectral correlation function (SCF) comparing the similarity between neighbouring spectra (Rosolowsky et al. 1999). When looking for characteristic global features in the density-velocity structure the principal component analysis (PCA) introduced by Heyer & Schloerb (1997) is probably the most significant tool. It identifies the main components in the position-velocity space in terms of eigenvectors and eigenimages. Although the PCA represents a reliable method to find the dominant main structures even in complicated images the significance of the higher-order moments still has to be tested. PCA and SCF are discussed in more detail by Vázquez-Semadeni (this volume).

A closure of the circle staring with the clump decomposition methods discussed in Sect. 3 is provided by the analysis of Tauber (1996). He discussed the smoothness of line profiles as a measure for the size and number of coherent units contributing to the line profiles. Applying a rough approximation of this type of analysis Falgarone et al. (1998) conclude that the size of cells in the Polaris Flare observations should be as low as 200 AU.

6 Conclusions

At the moment, we still do not know which physical meaning is hidden in the large zoo of measurable structure parameters. Most of them enlighten special aspects of structure formation and can help to discriminate between different simulations of molecular cloud structure. Only a small part of the information on the cloud structure is contained in the isotropic intensity structure. Anisotropy and the velocity space have to be investigated with the same effort.

Any model designed to fit the observed properties of molecular cloud has to reproduce many parameters and a large effort is required to provide a careful comparison between observations and models. The iterative process of the construction of models fitting more and more of the observational parameters will help to reveal the physical nature of turbulence in molecular clouds. Main discoveries on the cloud physics are to be expected from observations showing a deviation from self-similar scaling relations.

Acknowledgments

We thank A. Heithausen and E. Vázquez-Semadeni for helpful discussions. This work was supported by the Deutsche Forschungsgemeinschaft through grant SFB 301. The research has made use of NASA's Astrophysics Data System Abstract Service.

References

1. Adams F.C. & Wiseman J.J., *ApJ* **435**, 693 (1994)
2. Bensch F., Stutzki J. & Ossenkopf V., *A&A* **submitted**, (1999)
3. Blitz L. & Williams J.P., *ApJ* **488**, L145 (1997)
4. Chappell D.W. & Scalo J.M., *AAS* **180**, 2406 (1992)
5. Dame T.M., in *The Physics and Chemistry of the Interstellar Medium*, ed. Ossenkopf V., Stutzki J. & Winnewisser G., GCA-Verlag Herdecke (1999), p. 100
6. Falgarone E., Phillips T.G. & Walker C.K., *ApJ* **378**, 186 (1991)
7. Falgarone E., Lis D., Phillips T., Pouqet A., Porter D. & Woodward P., *ApJ* **436**, 728 (1994)
8. Falgarone E., Panis J.-F., Heithausen A., Pérault M., Stutzki J., Puget J.-L. & Bensch F., *A&A* **331**, 669 (1998)
9. Forbes D.A. & Thomson R.C., *MNRAS* **254**, 723 (1992)
10. Goodman A.A., Barranco J.A., Wilner D.J. & Heyer M.H., *ApJ* **504**, 223 (1998)

11. Heithausen A. & Thaddeus P., *ApJL* **353**, L49 (1990)
12. Heithausen A., Bensch F., Stutzki J., Falgarone E. & Panis J.F., *A&A* **331**, L65 (1998)
13. Heyer M.H. & Schloerb F.P., *ApJ* **475**, 173 (1997)
14. Houlahan P. & Scalo J., *ApJ* **393**, 172 (1992)
15. Juvela M., in *The Physics and Chemistry of the Interstellar Medium*, ed. Ossenkopf V. et al., GCA-Verlag Herdecke (1999), p. 220
16. Kleiner S.C. & Dickman R.L., *ApJ* **295**, 466 (1985)
17. Langer W.D., Wilson R.W. & Anderson C.H., *ApJ* **408**, L45 (1993)
18. Larson R.B., *MNRAS* **194**, 809 (1981)
19. Lis D.C., Keene J., Li Y., Phillips T.G. & Pety J., *ApJ* **504**, 889 (1998)
20. Mac Low M.-M., Klessen R.S., Burkert A. & Smith M.D., *Phys. Rev. Lett.* **80**, 2754 (1998)
21. Mac Low M.-M. & Ossenkopf V., *A&A* **submitted**, (1999)
22. Miesch M.S. & Scalo J.M., ApJ **450**, L27 (1995)
23. Miesch M.S., Scalo J. & Bally J., *ApJ* **submitted**, (1999)
24. Ossenkopf V., Bensch F. & Zielinsky M., in *Interstellar Turbulence*, ed. Franco J. & Carraminana A., Cambridge Univ. Press (1998)
25. Ossenkopf V., Bensch F., Mac Low M.-M. & Stutzki J., in *The Physics and Chemistry of the Interstellar Medium*, ed. Ossenkopf V., Stutzki J. & Winnewisser G., GCA-Verlag Herdecke (1999), p. 216
26. Ostriker E., in *Interstellar Turbulence*, ed. Franco J. & Carraminana A., Cambridge Univ. Press (1998)
27. Padoan P., Juvela M., Bally J. & Nordlund A. *ApJ* **504**, 300 (1998)
28. Rosolowsky E.W., Goodman A.A., Wilner D.J. & Williams J.P., *ApJ* **submitted**, (1999)
29. Stenholm L.G., *A&A* **137**, 133 (1984)
30. Stutzki J. & Güsten R., *ApJ* **356**, 513 (1990)
31. Stutzki J., Bensch F.,Heithausen A., Ossenkopf V. & Zielinsky M., *A&A* **336**, 697 (1998)
32. Vogelaar M.R. & Wakker B.P., *A&A* **291**, 557 (1994)
33. Tauber J.A., *A&A* **315**, 591 (1996)
34. Vázquez-Semadeni E., Ostriker E.C., Passot T., Gammie C.F. & Stone J.M., in *Protostars and Planets IV*, ed. Mannings V., Boss A. & Russel S., Univ. Arizona Press (1999)
35. Williams J.P., de Geus E.J. & Blitz L, *ApJ* **428**, 693 (1994)
36. Williams J.P., Blitz L. & Mc Kee C.F., in *Protostars and Planets IV*, ed. Mannings V., Boss A. & Russel S., Univ. Arizona Press (1999)
37. Wiseman J.J. & Adams F.C., *ApJ* **435**, 708 (1994)
38. Zimmermann T. & Stutzki J., *Fractals* **1**, 930 (1993)